IOPscience iopscience.iop.org

Home Search Collections Journals About Contact us My IOPscience

Experimental and theoretical investigation of the $4f^n \leftrightarrow 4f^{n-1}5d$ transitions in $YPO_4:Pr^{3+}$ and $YPO_4:Pr^{3+}$, Ce^{3+}

This article has been downloaded from IOPscience. Please scroll down to see the full text article.

2001 J. Phys.: Condens. Matter 13 765

(http://iopscience.iop.org/0953-8984/13/4/322)

View the table of contents for this issue, or go to the journal homepage for more

Download details:
IP Address: 171.66.16.226
The article was downloaded on 16/05/2010 at 08:25

Please note that terms and conditions apply.

INSTITUTE OF PHYSICS PUBLISHING JOURNAL OF PHYSICS: CONDENSED MATTER

J. Phys.: Condens. Matter **13** (2001) 765–776 www.iop.org/Journals/cm PII: S0953-8984(01)15985-0

Experimental and theoretical investigation of the $4f^n \leftrightarrow 4f^{n-1}5d$ transitions in $YPO_4:Pr^{3+}$ and $YPO_4:Pr^{3+}$, Ce^{3+}

M Laroche[1], S Girard[1], J Margerie[1], R Moncorgé[1,4], M Bettinelli[2] and E Cavalli[3]

[1] Centre Interdisciplinaire de Recherche Ions Lasers, UMR 6637 CEA-CNRS-ISMRA, Université de Caen, 6 Boulevard Maréchal Juin, 14050 Caen, France
[2] Dipartimento Scientifico e Tecnologico, Università di Verona, Ca' Vignal, Strada Le Grazie 15, 37134 Verona, Italy
[3] Dipartimento di Chimica Generale ed Inorganica, Chimica Analitica e Chimica Fisica, Università di Parma, Parco Area delle Scienze 17/A, 43100 Parma, Italy

E-mail: moncorge@spalp255.ismra.fr

Received 1 August 2000, in final form 11 November 2000

Abstract

Excited state absorption spectra from the $4f^2$ levels of Pr^{3+} in YPO_4 to 4f5d were measured at 293 and 77 K using a pulsed pump–probe technique. The spectra from the $^1D_2$ manifold were recorded by employing a continuous wave probe, whilst those from the ^3P_J–$^1I_6$ states were recorded by using for the first time a pulsed probe. These experimental results are compared with the numerical predictions of a full calculation of the 4f5d levels and the agreement is found to be good. A detailed study of the UV luminescence properties of the Pr^{3+} and the Ce^{3+} ions in the YPO_4 host crystal, including the energy transfer between these two ions, is also reported. Fluorescence spectra and decay curves from the lower excited-state levels of the 4f5d and 5d electronic configurations of the Pr^{3+} and Ce^{3+} ions, respectively, were measured both at 293 and 77 K. The $Pr^{3+} \rightarrow Ce^{3+}$ energy transfer efficiency was evaluated. Further considerations about the possibility to obtain laser emission based on the $5d \rightarrow 4f$ optical transition seem to indicate that this material is probably not a very good candidate to build a UV tunable laser because of a relatively short lifetime of the emitting level corresponding to a reduced quantum efficiency.

1. Introduction

It has been demonstrated that the $4f^{n-1}5d \rightarrow 4f^n$ broadband luminescence transitions of trivalent lanthanide rare earth ions can be useful for new tunable all-solid-state lasers in the blue and UV spectral domains (see for instance [1]). Considerable successes have been obtained in the case of materials doped with the Ce^{3+} ion, and it has been shown that several crystals

[4] Author to whom all correspondence should be addressed.

0953-8984/01/040765+12$30.00 © 2001 IOP Publishing Ltd Printed in the UK

can lead to reliable and efficient tunable UV coherent sources [2–8]. However, it is necessary to pump these materials with UV sources, which can lead to colour centre formation and very detrimental optical losses, and their laser emissions are at the moment limited to the near UV between about 280 and 335 nm [9, 10]. So, it is important to investigate other rare-earth doped crystals which can give rise to complementary UV emission domains and which can be pumped using different schemes. From this point of view, crystals doped with Pr^{3+} or codoped with Pr^{3+} and Ce^{3+} seem to be very attractive.

Pr^{3+} doped materials are in general interesting, even though no laser action has been obtained for them so far [11]. In fact, the states belonging to the 4f5d configuration can be pumped sequentially, using the $4f^2$ energy levels as intermediate steps, with blue/visible pump photons. As in the case of the 5d configuration of Ce^{3+}, the splitting of the energy levels of the 4f5d configuration of Pr^{3+} strongly depends on its surroundings. It is therefore important to understand the influence of the host crystal on the 4f5d configuration.

To this purpose, numerous energy levels belonging to this configuration have been located, employing excited state absorption (ESA) measurements, in oxide and fluoride crystals such as $YAlO_3$, KY_3F_{10}, BaY_2F_8 and $LiYF_4$ [12, 13]. In the case of the last material the experimental results have been recently compared with the numerical predictions of a full calculation of the 4f5d sublevels, and a good agreement has been obtained [14]. This investigation has shed light on the nature of the interactions mainly affecting the structure of the 4f5d configuration in fluoride crystals.

It is interesting to extend these studies to other crystalline materials doped with the Pr^{3+} ion. In particular, oxide hosts have been investigated in less detail both from an experimental and a theoretical point of view. It is also interesting to investigate the possible excitation of the luminescence of Ce^{3+} through an energy transfer process from the 4f5d configuration of Pr^{3+}, which can be populated by a two step absorption process using levels of the $4f^2$ configuration as intermediate states. This process has been recently evidenced in a codoped Cs_2NaYCl_6 crystal [15].

It was already reported in the 1960s that intense $5d \rightarrow 4f$ luminescence, with a quantum efficiency of 30%, is observed following UV excitation of YPO_4:Ce^{3+} [16]. This study was followed by several other papers dealing with the spectroscopy and the energy levels of this material [17–19]. However, to the best of our knowledge, the f–d transitions of YPO_4:Pr^{3+} have been only mentioned in a paper describing the cascade fluorescent decay in Pr^{3+} doped fluorides [20] and in a short paper describing the x-ray excited emission spectra of YPO_4:Pr^{3+} [21]. On the other hand, the f–f transitions of this material are well known. In fact, the crystal field parameters relative to the $4f^2$ configuration [22], and the decay rates of the $^3P_0$ [23] and $^1D_2$ [24] states have been reported for the Pr^{3+} ion in YPO_4.

For this reason, we decided to undertake a detailed investigation of the $4f^2 \leftrightarrow 4f5d$ spectroscopy of Pr^{3+}, and of the energy transfer processes from Pr^{3+} to Ce^{3+}, in the oxide crystal YPO_4. We report here the absorption and emission spectra recorded in the UV spectral region of YPO_4:Pr^{3+}, YPO_4:Ce^{3+} and YPO_4:Pr^{3+}, Ce^{3+} single crystals using single photon excitations and excited state absorption from both ^3P_J–$^1I_6$ and $^1D_2$. The experimental results are compared with the numerical predictions obtained from a full calculation of the 4f5d sublevels. We also report fluorescence decay measurements for each of the Pr^{3+} and Ce^{3+} emissions in the singly doped and co-doped samples. The efficiency of the energy transfer from Pr^{3+} to Ce^{3+} is evaluated.

2. Experiment

YPO_4 crystallizes in the $I4_1/amd$ (D_{4h}^{19}) tetragonal space group and the Y^{3+} ion occupies sites of D_{2d} symmetry surrounded by eight oxygen atoms [25]. We can note that the point group

symmetry is very close to the one of $LiYF_4$ (S_4) and it will be interesting to compare the results obtained for the two materials doped with Pr^{3+}. YPO_4 crystals nominally doped with 1 mol% Pr^{3+} or 1 mol% Ce^{3+}, and codoped with 1 mol% Pr^{3+} and 1 mol% Ce^{3+} (all with respect to Y^{3+}) were grown using the flux growth method employing $Pb_2P_2O_7$ as a solvent [26] in the 1300–800 °C temperature range. The charge composition was, in mol%: 50 $NH_4H_2PO_4$, 48 PbO, 2 Y_2O_3. The dopants were added as CeO_2 and/or Pr_6O_{11}. The Pt crucible containing the charge was heated at a rate of about 15–20 °C h^{-1} to 1300 °C in a horizontal furnace under air atmosphere. After a soaking time of 18 h, the temperature was lowered to 900 °C at a rate of about 2 °C h^{-1}. The crucible was then drawn out from the furnace and quickly inverted to separate from the flux the crystals grown at the bottom of the crucible. Single crystals of about $0.7 \times 0.7 \times 5$ mm^3 were used for the spectroscopic measurements.

For the excitation into the Ce^{3+} 5d levels in the $YPO_4:Ce^{3+}$ sample, a Ce:LiSAF laser pumped by a quadrupled Nd:YAG laser (Thomson-Laser model Diva II) was used. The output signal from this laser was tuned around 300 nm in order to obtain the maximum fluorescence. The Pr^{3+} ion was indirectly pumped step by step via the ^3P_J–$^1I_6$ levels by using the radiation of a wideband optical parametric oscillator (GWU model C355) with the signal tuned at $\lambda_1 = 480$ nm and part of the pump residue at $\lambda_2 = 355$ nm as described elsewhere [13]. This exciting radiation first populates the ^3P_J–$^1I_6$ levels and then excited state absorption allows us to populate the 4f5d states. The luminescence was collected and analysed through a monochromator (Jobin–Yvon Triax 550) equipped with a 1200 gr mm^{-1} grating blazed at 300 nm. The luminescence signal was detected with a photomultiplier tube (Hamamatsu model R3896). Lifetime measurements were carried out using a fast digital oscilloscope (Tektronix TDS 350) and fluorescence spectra were recorded after averaging by means of a boxcar integrator interfaced with a PC.

The ESA spectra originating from $^1D_2$ were recorded using the experimental set-up described elsewhere [13] where the lenses were replaced with uncoated aluminized concave mirrors to suppress chromatic aberrations. However, it was impossible to use the same technique for the ESA spectra originating from the ^3P_J–$^1I_6$ due to the very short lifetime of these states and the overlap with the ESA from $^1D_2$. We then replaced the continuous wave xenon lamp [13] by a pulsed short arc xenon lamp (Hamamatsu L2436) synchronized with the laser source and used the photomultiplier tube without preamplifier but with a load resistor of 50 Ω. The acquisition of the signal was carried out using the digital oscilloscope interfaced with a PC, which computes the curves after averaging over 16 samples.

3. Results and discussion

3.1. ESA spectra

The polarized ESA spectra recorded at 293 K after excitation into ^3P_J–$^1I_6$ and $^1D_2$ are shown in figures 1(a) and (b) and 2(a) and (b). If we compare these spectra with those obtained for $LiYF_4$ [13], we note that the structure in the two cases is clearly different. The first ESA band is located at a longer wavelength, i.e. around 405 nm (24 690 cm^{-1}) for the ESA spectra from $^3P_0$ for YPO_4, compared to 365 nm (27 400 cm^{-1}) in the case of $LiYF_4$, and at 360 nm (27 780 cm^{-1}) from $^1D_2$ for YPO_4 compared to 335 nm (29 850 cm^{-1}) for $LiYF_4$. This observation suggests a larger splitting and a stronger crystal field (CF) acting on the 5d electron in YPO_4, as confirmed by the fact that the observed features appear to be more spaced in the ESA spectra of this material. It is also evident that the two bands at the lowest energies in the ESA spectra from $^1D_2$ are characterized by asymmetrical shapes, with a tail on the short wavelengths side. This behaviour will be explained below.

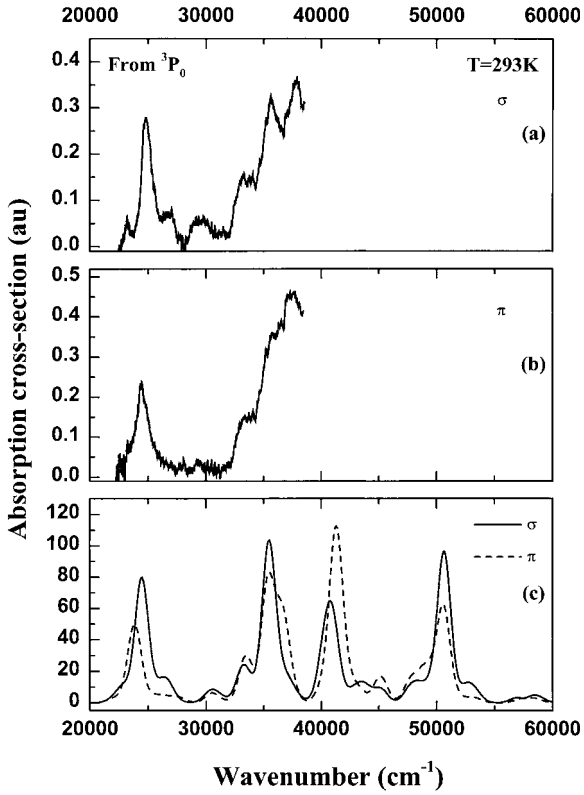

Figure 1. 293 K polarized ESA spectra from the ^3P_J–$^1I_6$ states of YPO_4:Pr^{3+}. (a) and (b) are the experimental spectra, whilst (c) shows the spectra predicted on the basis of the CF calculation.

Polarization effects are evident in the σ and π ESA spectra originating from the same level. This clearly indicates that selection rules are operative and that states characterized by different crystallographic quantum numbers μ are involved in the electric dipole transitions.

In order to improve the spectral resolution and to evidence the fine structure of the bands, ESA spectra were also recorded at low temperature. These measurements were carried out only at 77 K, since it has been shown that cooling at 8 K did not give rise in similar systems to a further improvement in the spectral resolution [14, 18]. However, low temperature measurements were carried out only from $^1D_2$ because ESA spectra registered from $^3P_0$ were too noisy to resolve the sharp line structure.

Figure 3 shows the 77 K polarized ESA spectra originating from the $^1D_2$ level. As for $LiYF_4$ [14], the low temperature spectra can be divided in two spectral domains, below or above 32 500 cm^{-1}. The low wavenumber domain of the spectra is characterized by very well resolved features (figure 4), whilst no sharp lines are evident in the high wavenumber region. This behaviour is probably due to a larger displacement of the potential energy curves of the excited states lying higher than 32 500 cm^{-1} above $^1D_2$. In any case, whilst eight zero-phonon lines were identified in the low temperature ESA spectra from $^1D_2$ in the case of $LiYF_4$:Pr^{3+} [14], only four sharp zero-phonon lines can be unambiguously located for YPO_4:Pr^{3+}.

We point out that in the present spectra each zero-phonon line is accompanied by a reasonably well resolved fine structure spreading about 700–900 cm^{-1} at higher energies. These sharp features collapse into a relatively broad and unresolved band when the crystal is

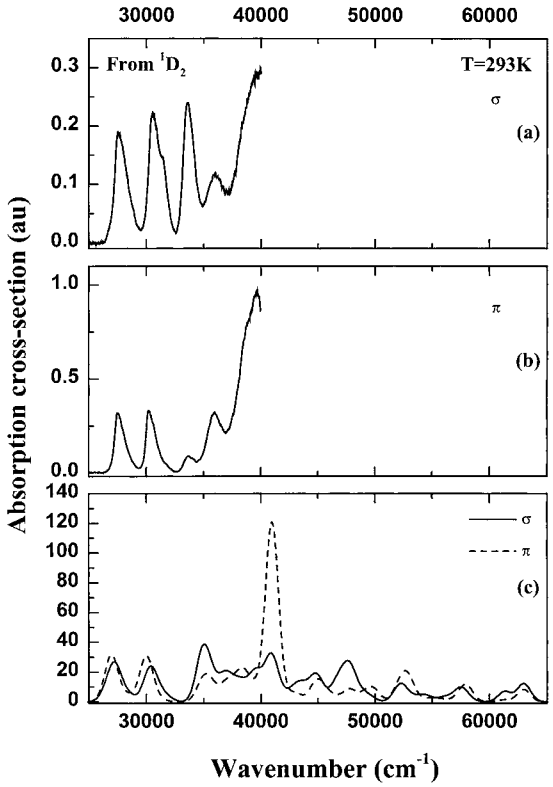

Figure 2. 293 K polarized ESA spectra from the $^1D_2$ state of $YPO_4:Pr^{3+}$. (a) and (b) are the experimental spectra, whilst (c) shows the spectra predicted on the basis of the CF calculation.

heated up to room temperature, therefore explaining the observed asymmetrical shape in the 293 K spectra. The fine structure is composed of sharp features whose intensity decreases moving away from the zero-phonon lines. This sideband can be safely assigned to a weak progression in a vibrational mode of about 150 cm^{-1}, although other features located about 500–800 cm^{-1} above the zero-phonon lines can be identified. The mode at 150 cm^{-1} could be due to a total symmetric localized vibration of the PrO_8 polyhedra. In fact, relatively intense features were found in the 130–180 cm^{-1} region of the Raman spectrum of PrPO4 [27]; however they were not assigned, and we also note that $PrPO_4$ has a crystal structure different from that of YPO_4.

The vibrational progression in the 150 cm^{-1} mode extends with measurable intensity only for two or three members. This clearly indicates that the displacement of the potential energy curve of the excited state, relative to the $4f^2$ ground state, is relatively small for the two 4f5d lowest energy levels reached by ESA from $^1D_2$. This agrees with the small difference in energy between the spectral position of the zero-phonon line and the maximum of the associated absorption band in the room temperature spectra. This difference can be evaluated to be lower than 150 cm^{-1} but there is no point in measuring an accurate value.

It is interesting to note that the sidebands of the f–d transitions of $YPO_4:Pr^{3+}$ are not dominated by vibrational modes relative to the PO_4^{3-} ion. This behaviour is different from that observed in the case of the f–d absorption and emission transitions of $YPO_4:Ce^{3+}$ [18]. The reasons for this different behaviour have to be ascertained.

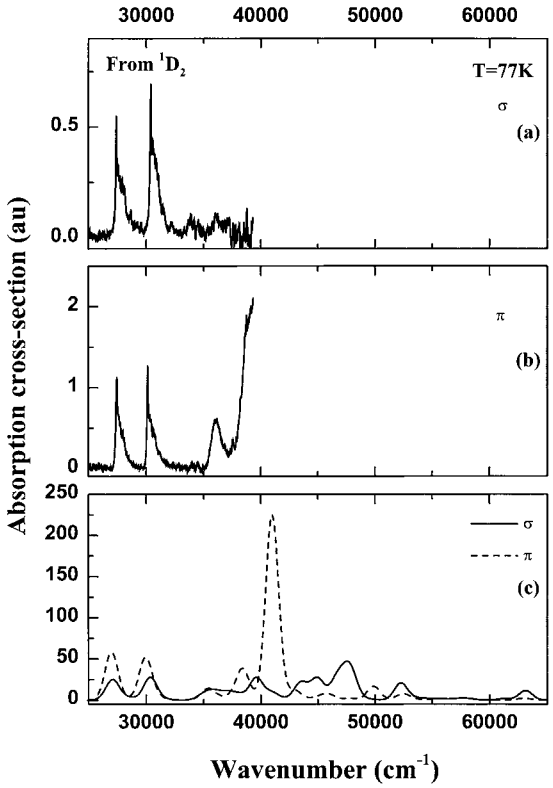

Figure 3. 77 K polarized ESA spectra from the $^1D_2$ state of $YPO_4:Pr^{3+}$. (a) and (b) are the experimental spectra, whilst (c) shows the spectra predicted on the basis of the CF calculation.

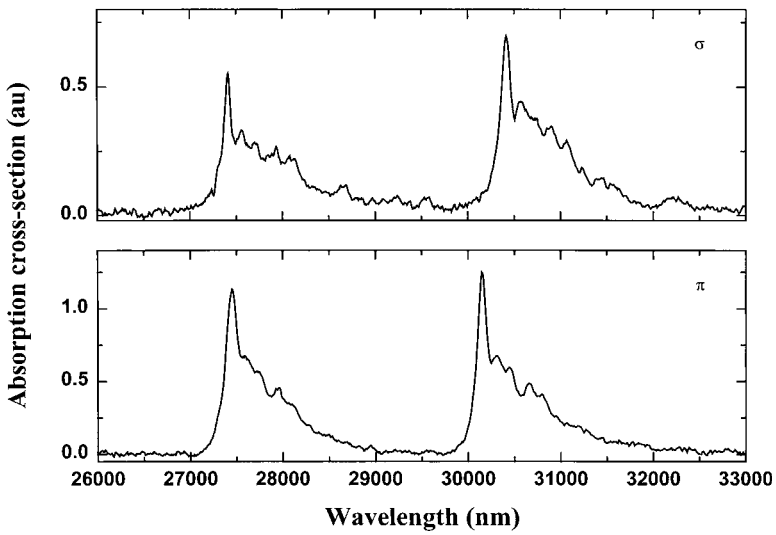

Figure 4. Enlargement of the two lowest energy ESA bands from the $^1D_2$ state of $YPO_4:Pr^{3+}$ at 77 K.

3.2. Crystal field calculations

Numerical predictions of the $4f^2 \rightarrow 4f5d$ optical transitions, derived from a full calculation of the 4f5d sublevels, have been previously carried out in the case of $LiYF_4$ [14]. We decided to perform the same calculations for YPO_4 in order to understand how the substitution of fluoride with oxide ligands can modify the crystal field. The D_{2d} point symmetry of the Pr^{3+} ion in YPO_4 is such that only the parameters B_{20}, B_{40} and B_{44} have to be considered in the CF Hamiltonian for the 4f5d configuration. In the present calculations, three quantities were taken as adjustable, i.e. the CF parameters $B_{20}(5d)$ and $B_{40}(5d)$ and the free ion parameter F_0, which shifts the 4f5d configuration as a whole [14]. $B_{44}(5d)$ was then calculated using the approximate relation:

$$B_{44}(5d) = \frac{B_{44}(4f)B_{40}(5d)}{B_{40}(4f)}.$$

The values of the CF parameters for the $4f^2$ configuration were taken from previous calculations [22]. The basics for the eigenstate calculation and the simulation of the ESA spectra have been described elsewhere [14]. The two ratios between $B_{kq}(4f)$ and $B_{kq}(5d)$ (for $k = 2$ and $k = 4$, respectively) which had been obtained for $LiYF_4:Pr^{3+}$ were used first but did not yield good results when the experimental and theoretical spectra were compared. For this reason, the two parameters $B_{20}(5d)$ and $B_{40}(5d)$ were first varied in a wide domain until we obtained simulated spectra that were similar to the experimental ones. In order to produce the best fit to the experimental positions of electric dipole transitions, we have to locate these transitions carefully. The main conditions to take into account to retain a particular peak for the comparison is that only one theoretical transition corresponds to the position of the peak, that the transition is intense and that it does not overlap too much with another one. Following this procedure, we chose ten transitions, in particular four corresponding to zero-phonon lines belonging to the ESA spectra from $^1D_2$ and six corresponding to the maximum of relatively broad features in the ESA spectra from both $^1D_2$ or $^3P_0$. The positions of the identified transitions are reported in table 1 together with their assignments in terms of the crystallographic quantum number μ. As for the free ion parameters, we used the same ones as for $LiYF_4$ [14], whilst the values of the five $B_{kq}(4f)$ parameters were calculated by Hayhurst *et al* [22]. The optimum FWHM for the simulation of the ESA spectra was found to be equal to 1300 cm^{-1}. The calculation gives the following parameters:

$$F_0 = 59\,743\ cm^{-1} \qquad B_{20}(5d) = B_{20}(4f) \times 8.0 = 624.8\ cm^{-1}$$
$$B_{40}(5d) = B_{40} \times 37.5 = 12\,040.7\ cm^{-1} \qquad B_{44}(5d) = B_{44}(4f) \times 37.5 = -31\,846\ cm^{-1}.$$

The proportionality constant between $B_{4q}(4f)$ and $B_{4q}(5d)$ is at least two times larger than those previously obtained for Pr^{3+} or Ce^{3+} in fluoride crystals [14, 28]; this could explain the larger 4f5d splitting observed for YPO_4. The effective value of F_0, which is found in these calculations, is significantly lower than the one calculated for $LiYF_4:Pr^{3+}$ [14]. This behaviour could be explained both by the fact that this quantity decreases by embedding the Ln^{3+} ion in a host [29], and that it contains the $B_{00}(5d)$ parameter, which depends on the crystal field at the Ln^{3+} site.

The calculated room temperature ESA spectra are presented in figures 1 and 2. The overall qualitative agreement with the experimental spectra is good, apart from some differences in the positions of the various bands. The fact that it is impossible to fit perfectly the whole set of ESA bands seems to derive from differences between the two spectra mentioned above (section 3.1). In fact, a different coupling with lattice vibrations for the excited states belonging to the two spectral domains could explain the disappearance of zero-phonon lines in the high wavenumber domain (because of a larger displacement of the minima of the potential curves

Table 1. Energy positions and assignments of the f–d bands used in the calculation of the ESA spectra of YPO_4:Pr^{3+}.

Initial state polarization	Position		Identification	
	Calculated (cm^{-1})	Observed (cm^{-1})	Start level	End level
From $^1D_2$				
π polarized	26 983	27 450	$^1D_2, \mu = 2$	$\mu = 2$
	29 934	30 170	$^1D_2, \mu = 2$	$\mu = 2$
	34 894	33 784	$^1D_2, \mu = \pm 1$	$\mu = \pm 1$
σ polarized	27 060	27 424	$^1D_2, \mu = 2$	$\mu = \pm 1$
	30 342	30 437	$^1D_2, \mu = 2$	$\mu = \pm 1$
	34 837	33 613	$^1D_2, \mu = 0$	$\mu = \pm 1$
From ^3P_J, $^1I_6$				
π polarized	23 898	24 426	$^3P_0, \mu = 0$	$\mu = 0$
	33 383	33 557	$^3P_0, \mu = 0$	$\mu = 0$
σ polarized	24 455	24 814	$^3P_0, \mu = 0$	$\mu = \pm 1$
	33 141	33 557	$^3P_0, \mu = 0$	$\mu = \pm 1$

of the relevant excited states). We point out that these two domains also show a different static coupling with the lattice which is evidenced by different splittings. The observation that an absorption band from $^1D_2$, belonging to the high wavenumber domain in σ polarization, almost disappears at low temperature can be explained on the basis of the CF calculations. In fact, they show that the starting level of the disappearing ESA band is the third Stark component of the $^1D_2$ state, lying at 214 cm^{-1} above the lowest CF state. This second level is thermally populated at 293 K, but its population drastically decreases at 77 K.

It is well known that oxide hosts are usually characterized by a stronger crystal field than fluorides. One way to evaluate and compare the strength of the crystal field in different materials is to use a definition given by Auzel [30].

$$N_V = \left[\sum_{k \neq 0, q} \frac{4\pi}{2k+1} (B_q^k)^2 \right]^{1/2}.$$

In the case of $LiYF_4$:Pr^{3+}, we found $N_v(4f^2) = 2387$ cm^{-1} whilst for YPO_4:Pr^{3+}, $N_v(4f^2) = 1731$ cm^{-1}, indicating that the CF acting on the 4f configuration is stronger for the former host. However, $N_v(4f5d)$ is 29 717 cm^{-1} for $LiYF_4$:Pr^{3+} and 40 243 cm^{-1} for YPO_4, suggesting that the trend is reversed for the 4f5d configuration. This peculiar effect is not explained so far and would need further investigations.

3.3. Luminescence properties and energy transfers

The room temperature fluorescence lifetime of the $^3P_0$ state of YPO_4:1% Pr^{3+} is 660 ns, corresponding to a decay rate of 1.5×10^6 s^{-1}. We note that cooling the sample at 77 K does not increase the value of the lifetime. This observation agrees with a simple model for the temperature dependence of the multiphonon relaxation rate [31]. The radiative lifetime of this state, evaluated using the Judd–Ofelt parameters [32], is 5.7 μs, corresponding to a decay rate of 1.8×10^5 s^{-1}. Non-radiative processes seem to be efficient in depopulating the $^3P_0$ state

towards, in part, the $^1D_2$ state as the fluorescence from this state is clearly stronger when, using the same pump energies, we pump the $^3P_0$ state instead of the $^1D_2$ state. It is possible to evaluate the multiphonon relaxation rate W_{nr} on the basis of a modified energy gap model [33]; using the parameters reported for phosphate glasses, and the maximum phonon energy of 1050 cm^{-1} reported for YPO_4 [27], we obtain $W_{nr} \approx 8 \times 10^4$ s^{-1}, yielding a calculated total decay rate of 2.6×10^5 s^{-1}, which is about one order of magnitude lower than the observed decay rate. However, it is important to note that the Judd–Ofelt scheme is particularly difficult to apply in the case of the Pr^{3+} ion, and that the values of W_{nr} obtained using the model described in [33] have to be considered as accurate within one to two orders of magnitude [34].

As explained previously [15], two-step excitation should be an efficient process to populate the 4f5d energy levels of Pr^{3+}, as the two absorption cross-sections should be relatively high. The ESA spectra from $^1D_2$ show that an absorption occur around 355 nm (28 170 cm^{-1}) in both polarizations. This pumping process was demonstrated by sending onto the $YPO_4:Pr^{3+}$ sample the output beam of the OPO at about 590 nm and a part of the pump residue at 355 nm, optically delayed by 5 ns. We obtained an emission spectrum exactly identical to the one shown by Naik *et al* [21]. On the other hand, at 77 K, no fluorescence could be detected by using the same excitation wavelengths, which suggests that the second step was not efficient enough, because of narrower ESA lines (figures 3 and 4).

The emission spectra of Ce^{3+} both at room temperature and 77 K are shown in figure 5 together with the absorption spectrum at 293 K. A Stokes shift of 1070 cm^{-1} can be evaluated, which is much less than the value given by Blasse and Bril (2800 cm^{-1}) [16]. The difference in energy between the spectral position of the zero-phonon line and the maximum of the associated emission band is not as small as for the ESA of Pr^{3+} (as discussed above) and is found to be near 550 cm^{-1} after averaging over the two emission bands. This value is about half of the Stokes shift, which shows that a mirror symmetry occurs between the emission and absorption band. This is confirmed by the width of the lowest energy absorption band and the highest energy emission band, that are very close (1165 and 1120 cm^{-1}).

The room temperature decay curves of the f–d luminescence of $YPO_4:Ce^{3+}$, $YPO_4:Pr^{3+}$ and $YPO_4:Pr^{3+}$, Ce^{3+} are shown in figure 6. As the pulse duration of the excitation is of the

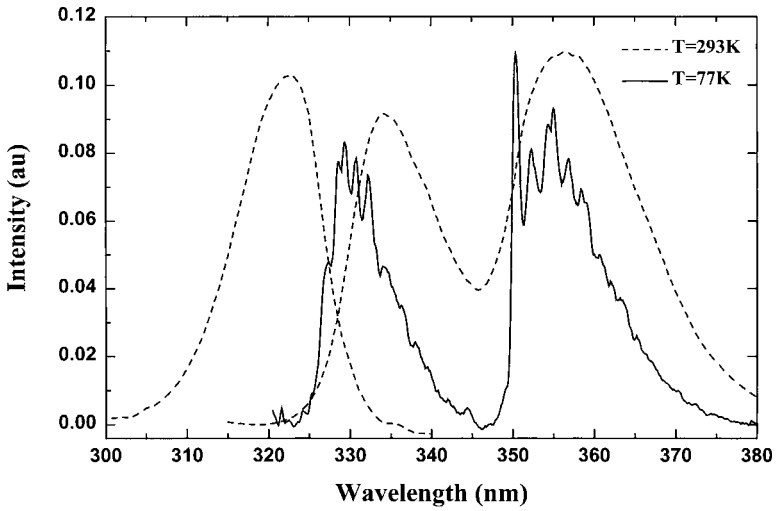

Figure 5. Absorption spectrum at 293 K (left) and emission spectra at 293 and 77 K (right) of $YPO_4:Ce^{3+}$.

order of a few nanoseconds, it is difficult to deconvolute the experimental decay curves in order to obtain precise experimental lifetimes. However, it is possible to estimate that for the singly doped YPO_4:Ce^{3+} crystal the lifetime of the excited state is 23 ns, whilst for YPO_4:Pr^{3+} the value of the lifetime is 17 ns. We note that, as usual, the lifetime of the lower d state is longer for Ce^{3+} than for Pr^{3+}. However, possibly due to non-radiative relaxation, these lifetimes appear to be shorter than in fluoride crystals such as $LiYF_4$ (26 and 40 ns respectively for Pr^{3+} and Ce^{3+}).

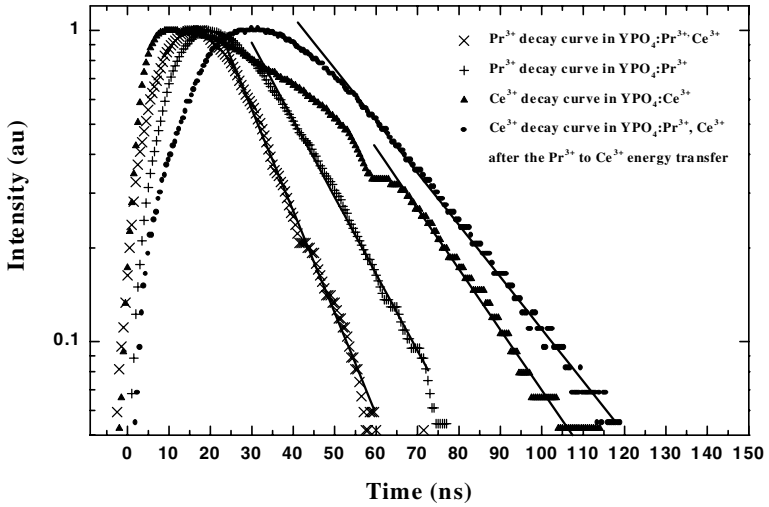

Figure 6. 293 K decay curves of the f–d luminescence of Ce^{3+} and Pr^{3+} in single-doped and codoped YPO_4; the solid lines represent a linear fit.

In the case of the codoped YPO_4:Pr^{3+}, Ce^{3+} crystal, the time evolution of the luminescence intensity of Ce^{3+} after pulsed excitation of the Pr^{3+} ion clearly shows the presence of a rise. Assuming an exponential decay for the Pr^{3+} luminescence in the codoped crystal, the lifetime of the excited state decreases to 13 ns, whilst that of Ce^{3+} increases slightly to 25 ns, within the experimental uncertainties. These results clearly show the presence of energy transfer from the lowest state of the 4f5d configuration of Pr^{3+} to states belonging to the 5d configuration of Ce^{3+}, as also indicated by the fact that in the emission spectrum of the codoped crystal the Pr^{3+} emission appears to be quenched (figure 7). Bearing in mind the uncertainties associated with the present values of the decay times, it is possible to evaluate the efficiency of energy transfer. Assuming that the transfer probability is time independent, it is possible to use a simple formula to evaluate the transfer efficiency η on the basis of the lifetime for the donor state of Pr^{3+} in the singly doped crystal (τ_0) and in the codoped one ($\tau_{codoped}$):

$$\eta = 1 - \frac{\tau_{codoped}}{\tau_0}.$$

In the codoped YPO_4:Pr^{3+}, Ce^{3+} crystal, the efficiency η is about 24%. We point out that this energy transfer is a very important issue for lasing Ce^{3+} doped crystals by pumping with visible photons.

4. Conclusions

In this paper we have presented a detailed investigation of the interconfigurational f–d transitions of Pr^{3+} and Ce^{3+} in single crystals of YPO_4, using absorption, luminescence and

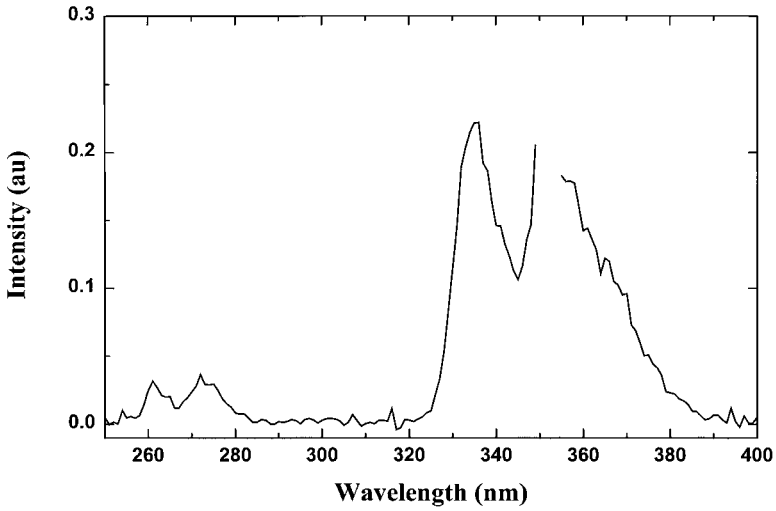

Figure 7. 293 K emission spectra of Pr^{3+} and Ce^{3+} codoped YPO_4 after two-step excitation (via $^3P_J - ^1I_6$). Note: only the two lowest energy emission bands are shown for Pr^{3+}. The hole in the emission bands of Ce^{3+} is due to the excitation at 355 nm.

excited state absorption spectroscopy. The results have allowed us to obtain information on the electronic structure of the 4f5d configuration of Pr^{3+}, through the good agreement with the numerical predictions yielded by a full calculation of the 4f5d sublevels in a D_{2d} crystal field.

With respect to $LiYF_4$ in which Pr^{3+} occupies a site of similar symmetry, the crystal field acting on the 5d orbitals in YPO_4 appears to be significantly stronger. This results in a larger splitting, and in f–d absorption spectra which are more spread. The stronger crystal field partly explains the lower energy position of the f–d luminescence observed for YPO_4, compared to fluoride materials.

It has also been possible to demonstrate that the f–d luminescence of $YPO_4:Pr^{3+}$ can be obtained at room temperature through a two-step excitation scheme using pump photons in the visible and the near UV. Moreover, the same scheme yields emission from Ce^{3+} in the codoped crystals, through relatively efficient $Pr^{3+} \rightarrow Ce^{3+}$ energy transfer. However, due to the short lifetimes values of both the 5d and 4f5d luminescence of Ce^{3+} and Pr^{3+} ions in this material, it is doubtful that these systems can be considered as a potential candidate for the development of tunable lasers in the UV spectral region.

References

[1] Hooker S M and Webb C E 1994 *Prog. Quantum Electron.* **18** 227
[2] Erlich D J, Moulton P F and Osgood R M Jr 1979 *Opt. Lett.* **4** 184
[3] Erlich D J, Moulton P F and Osgood R M Jr 1980 *Opt. Lett.* **5** 339
[4] Dubinskii M A, Semashko V V, Naumov A K, Abdulsabirov R Y and Korableva S L 1993 *J. Mod. Opt.* **40** 1
[5] Marshall C D, Speth J A, Payne S A, Krupke W F, Quarles G J, Castillo V and Chai B H T 1994 *J. Opt. Soc. Am.* B **11** 2054
[6] Pinto J F, Rosenblatt G H, Esterowitz L and Quarles G J 1994 *Electron. Lett.* **30** 240
[7] Liu Z, Ohtake H, Sarukura N, Dubinskii M, Abdulsabirov R Y and Korableva S L 1998 *Advanced Solid State Lasers (OSA TOPS Vol. 19)* ed W R Bosenberg and M J Fejer (Optical Society of America) p 13
[8] Rambaldi P, Moncorgé R, Wolf J P, Pédrini C and Gesland J Y 1998 *Opt. Commun.* **146** 163
[9] Govorkov S V, Wiessner A O, Schröder T, Stamm U, Zschocke W and Basting D 1998 *Advanced Solid State Lasers (OSA TOPS Vol. 19)* ed W R Bosenberg and M J Fejer (Optical Society of America) p 2

[10] McGonigle A J S, Girard S, Coutts D W and Moncorgé R 1999 *Electron. Lett.* **35** 1640
[11] Lawson J K and Payne S A 1993 *Opt. Mat.* **2** 225
[12] Nicolas S, Laroche M, Girard S, Moncorgé R, Guyot Y, Joubert M F, Descroix E and Petrosyan A G 1999 *J. Phys.: Condens. Matter* **11** 7937
[13] Laroche M, Braud A, Girard S, Doualan J L, Moncorgé R and Thuau M 1999 *J. Opt. Soc. Am.* B **16** 2269
[14] Laroche M, Doualan J L, Girard S, Margerie J and Moncorgé R 2000 *J. Opt. Soc. Am.* B **17** at press
[15] Laroche M, Bettinelli M, Girard S and Moncorgé R 1999 *Chem. Phys. Lett.* **311** 167
[16] Blasse G and Bril A 1967 *J. Chem. Phys.* **47** 5139
[17] Hoshina T and Kuboniwa S 1971 *J. Phys. Soc. Japan* **31** 828
[18] Nakazawa E and Shionoya S 1974 *J. Phys. Soc. Japan* **36** 504
[19] Sytsma J, Piehler D, Edelstein N, Boatner L A and Abraham M M 1993 *Phys. Rev.* B **47** 14 786
[20] Piper W W, DeLuca J A and Ham F S 1974 *J. Lumin.* **8** 344
[21] Naik R C, Kranjikar N P and Narasimham N A 1981 *Solid State Commun.* **38** 389
[22] Hayhurst T, Shalimoff G, Conway J G, Edelstein N, Boatner L A and Abraham M M 1982 *J. Chem. Phys.* **76** 3960
[23] Reed E D Jr and Moos H W 1973 *Phys. Rev.* B **8** 980
[24] Naik R C, Karanjikar N P and Razvi M A N 1992 *J. Lumin.* **54** 138
[25] Milligan W O, Mullica D F, Beall G W and Boatner L A 1982 *Inorg. Chim. Acta* **60** 39
[26] Feigelson R S 1964 *J. Am. Ceram. Soc.* **47** 257
[27] Begun G M, Beall G W, Boatner L A and Gregor W J 1981 *J. Raman Spectrosc.* **11** 273
[28] Apaev R A, Eremin M V, Naumov A K, Semashko V V, Abdulsabirov R Yu and Korableva S L 1998 *Opt. Spektrosk.* **84** 816
[29] Reisfeld R and Jorgensen C K 1977 *Lasers and Excited States of Rare Earths* (Berlin: Springer) p 124
[30] Auzel F 1980 *Radiationless Processes* ed B DiBartolo and V Goldberg (New York: Plenum) p 213
[31] Riseberg L A and Moos H W 1968 *Phys. Rev.* B **174** 429
[32] Savardi C 1999 *Tesi di Laurea* Università di Parma
[33] van Dijk J M F and Schuurmans M F H 1983 *J. Chem. Phys.* **78** 5317
[34] De Mello Donegá C, Meijerink A and Blasse G 1995 *J. Phys. Chem. Solids* **56** 673